CHAPTER 2

Fibroblasts from women with pelvic organ prolapse show differential mechanoresponses depending on surface substrates

A.M. Ruiz-Zapata
M.H. Kerkhof
B. Zandieh-Doulabi
H.A.M. Brölmann
T.H. Smit
M.N. Helder

Int Urogynecol. 2013 Sep: 24(9):1567-75

ABSTRACT

Introduction and hypothesis Little is known about dynamic cell-matrix interactions in the context of pathophysiology and treatments for pelvic organ prolapse (POP). This study sought to identify differences between fibroblasts from women with varying degrees of prolapse in reaction to mechanical stimuli and matrix substrates *in vitro*.

Methods Fibroblasts from the vaginal wall of three patients with POP-Quantification (POP-Q) system stages 0, II, and IV were stretched on artificial polymer substrates either coated or not coated with collagen I. Changes in morphology and anabolic/catabolic compounds that affect matrix remodelling were evaluated at protein- and gene expression levels. Statistical analysis was performed using one-way analysis of variance (ANOVA), followed by Tukey-Kramer's post hoc test.

Results POP fibroblasts show delayed cell alignment and lower responses to extracellular matrix remodelling factors at both enzymatic- and gene-expression levels compared with healthy fibroblasts.

Conclusion POP fibroblasts, when compared with healthy cells, show differential mechanoresponses on two artificial polymer substrates. This should be taken into account when designing or improving implants for treating POP.

INTRODUCTION

Pelvic organ prolapse (POP) is a common multifactorial disease with known risk factors and unclear pathogenesis. POP is characterized by weakening of the pelvic floor and is associated with serious inconveniences and reduced quality of life (QoL) in almost 50% of women >50 years of age. Conservative therapies are not always possible or sufficient, and reconstructive surgery with native tissue has high failure rates. Of all treated patients, 30% will experience recurrent POP within the first 2 years of treatment[1,2]. In the 1970s, urogynecologists began using polymeric meshes, originally designed to treat inguinal hernia, in an attempt to restore tissue support in POP patients. However, complications such as mesh contraction, exposure, or extrusion caused such serious health problems that in July 2011, the US Food and Drug Administration (FDA) issued a safety communication about the use of transvaginal mesh in POP repair[3,4]. Thus, improved therapies are urgently needed but their development are, however, hampered by a lack of understanding of the pathophysiology of the disease, along with sparse knowledge of the cause-effect relationships of mesh failure in patient tissue[5,6].

In recent years, there has been a growing interest in studying tissue composition of patients with prolapse. Researchers have mainly focused on characterizing the extracellular matrix (ECM) of connective tissue that support the pelvic floor, such as the vaginal wall[2,7–11], the uterosacral ligaments[12,13], and the pubocervical fascia[13,14]. Different outcomes have been reported, but the overall consensus is that the connective tissue of the vaginal wall is abnormal in women with POP[15]. The vaginal wall is one of the soft tissues that is constantly being remodelled so it can withstand the different forces applied to it during a woman's lifetime. Thus, weakening of the pelvic floor could be caused by an imbalance in its remodelling[2,7,8]. The presence of artificial substrates may very well influence this process.

Tissue remodelling is a well-balanced process involving several factors with different roles, with cells as modulators. In the vaginal wall, fibroblasts are mechanosensitive cells responsible for maintaining ECM homeostasis. They produce molecules and control anabolic and catabolic processes to remodel their surrounding matrix in response to mechanical and biochemical stimuli. Compounds particularly involved in ECM homeostasis include collagens (mainly types I and III), collagen-degrading matrix metalloproteinases (MMPs), and tissue inhibitors of metalloproteinases (TIMPs). MMPs are involved in both normal and pathological ECM remodelling processes throughout the body, including the pelvic floor. It has been shown that the amounts of active MMP-2[12,13,16] and/or MMP-9[7,17] are increased in tissue from patients with POP in comparison with controls. However, we were interested to see whether these MMPs are also increased when cells are exposed to cyclic mechanical loading. Furthermore, the question remains whether this enzymatic activity is affected by the presence of artificial polymeric substrates.

In order to answer these questions, our study was designed to evaluate *in vitro* dynamic cell-matrix interactions that are important for understanding the pathophysiology of and treatments for POP. We hypothesized that fibroblasts from women with different

degrees of prolapse display different mechanoresponses depending on the substrate encountered.

This hypothesis was tested by subjecting fibroblasts from healthy women and those with mild or severe POP to cyclic mechanical loading mimicking continuous respiration[18] on artificial polymeric membranes both uncoated and coated with collagen I. Changes in morphology and anabolic/catabolic compounds that may affect remodelling of the ECM were analyzed.

MATERIALS AND METHODS

Patient selection, tissue processing, and cell culture

Retrieval of biopsies was approved by the medical ethics committees of two hospitals in The Netherlands: VU University Medical Centre (Amsterdam) and Kennemer Gasthuis Hospital (Haarlem), and informed consent was obtained from all participants. Full-thickness biopsies (1 cm^2) of the anterior vaginal wall were obtained during vaginal hysterectomy of one patient with mild [POP Quantification (POP-Q) system, stage II] and one patient with severe POP (POP-Q stage IV). A third woman, who was operated for benign gynecological reasons, was selected as a healthy control. For ethical reasons, the biopsy site of the latter patient was the precervical region of the anterior vaginal wall. Tissues were collected in phosphate-buffered saline (PBS) at 4°C, and cells were isolated within 24h under sterile conditions. Fascia was scraped, cut into little pieces, and digested with Liberase TM (final concentration 0.3 U/ml; Roche Diagnostics, Mannheim, Germany) for 3h at 37°C and constant agitation. After filtration with a 100 μm cell strainer (BD Falcon, Franklin Lakes, NJ, USA), the pellet was resuspended in Dulbecco's modified Eagle's medium (DMEM) supplemented with 10% fetal bovine serum (FBS), 100 U/ml penicillin, 100 μg/ml streptomycin, and 250 μg/ml amphotericin-B. FBS was obtained from HyClone (South Logan, UT, USA); the other culture components were obtained from Gibco-Life Technologies (Paisley, UK) and Sigma (St. Louis, MO, USA). Subsequently, cells were seeded on six-well plates and grown in an incubator at 37°C, 95% humidity, and 5% carbon dioxide (CO_2) until they reached 60% confluence. At that point, the cells were considered to be at passage 0. Fibroblasts from passage 3–5 were used for loading experiments.

Cyclic mechanical loading

Forty-eight hours before mechanical loading, fibroblasts were seeded at a density of 150,000 cells/well on two artificial polymer substrates: six-well uncoated or collagen I-coated silicone Bioflex® plates (BioFlex, Flexcell International Corp., McKeesport, PA, USA). Just before loading, the cells were refreshed using culture media containing 1% FBS. The loading regime was applied using a Flexercell FX4000 system (Flexcell) and consisted of 24 or 48h of continuous cyclic mechanical loading (CML) mimicking continuous respiration, as described by Blaauboer and colleagues[18] (parameters: sinusoidal

wave, frequency 0.2 Hz, and maximum elongation 10%). The Flexercell device is widely used and has a vacuum pump that pulls down the elastic membrane of the bioflex plates, stretching the cells that are seeded on top accordingly. Fibroblasts cultured under the same conditions but without loading served as static controls. After the loading period, the cells were imaged using the bright field of an inverted Leica DMIL microscope with a DFC320 digital camera (Leica Microsystems, Wetzlar, Germany), and samples were collected for F-actin staining, MMP activity, protein content, and gene expression.

F-actin staining

For immunocytochemical staining of F-actin, cells were fixed using 4% formaldehyde, stained for F-actin with Alexa Fluor 488 phalloidin (Molecular Probes, Leiden, The Netherlands), and imaged using an inverted Leica DMIL microscope (Leica Microsystems), as previously described[19].

Enzymatic activity

After mechanical loading, conditioned media was collected, and the gelatinolytic activity of MMP-2 and MMP-9 was evaluated by zymography using 10% Novex zymogram gelatin gel (Life Technologies) following manufacturers' protocol. Dark bands of gelatinolytic activity were visualized using an eStain protein staining device (GeneScript, Piscataway, NJ, USA). Images were acquired with Biospectrum AC Imaging System (UVP, Cambridge, UK), and zymogram quantification of band density was performed using Image J 1.44p software (National Institutes of Health, USA). Quantitative data was normalized to total protein content (see below).

Western blot analysis

Conditioned media after 48h of loading were used to detect protein levels of TIMP-2 by Western blot. Samples were concentrated 2x by freeze drying, denatured for 5 min, and reduced with dithiothreitol. Samples were separated by electrophoresis on a NuPAGE® Novex 4-12% Bis-Tris gel and transferred to iBlot® polyvinylidene fluoride (PVDF) membrane (Life Technologies). For protein detection, monoclonal antibody anti-TIMP-2 mouse (mAb T2-101; Calbiochem®, Merck Millipore, Darmstadt, Germany) was used at a concentration of 1:500. Blots were blocked for 1h at room temperature with a blocking buffer [PBS with 0.5% Tween-20 and 1% bovine serum albumin (BSA)], then incubated with primary antibody in blocking buffer for 1h at room temperature, followed by overnight incubation at 4°C. Bound antibodies were visualized with a horseradish peroxidase-conjugated antibody goat anti-mouse (1:10,000) and Supersignal West Pico Chemiluminescent kit (Thermo Scientific, Rockford, IL, USA). Images were acquired with Biospectrum AC Imaging System (UVP), and quantification of band density was performed using Image J 1.44p software (NIH).

Total protein quantification

For total protein quantification, cells were lysed in buffer containing 50 mM Tris, pH 7.5, 150 mM sodium chloride (NaCl), 1 mM sodium orthovanadate, 1% Nonidet P-40, 0.1% sodium deoxycholate, and ethylenediaminetetraacetate (EDTA)-free protease inhibitor mixture (Sigma-Aldrich). Total protein content was determined using Pierce BCA Protein Assay kit (Thermo Scientific) following the supplier's specifications. Quantification was performed spectrophotometrically between 540-590 nm and using a 1,420 multilabel counter VICTOR^2 (WALLAC, Turku, Finland).

Gene expression

For gene expression, cells were lysed in a solution (1:100) of β-mercaptoethanol (Sigma-Aldrich) and RA1 buffer (Macherey-Nagel, Bioke, Leiden, The Netherlands). According to the manufacturers' instructions, total RNA was isolated using NucleoSpin TriPrep kit (Bioke) to a final concentration of 250 ng/ml and was reverse transcribed using SuperScript VILO complementary DNA (cDNA) synthesis kit (Life Technologies). Gene expression of alpha-1(I) procollagen (Col1a1), alpha-1(III)procollagen (Col3a1), matrix metalloproteinase-2 (MMP-2), TIMP-2, and the housekeeping genes tyrosine 3-monooxygenase/tryptophan 5-monooxygenase activation protein, zeta polypeptide (Ywhaz) and human ubiquitin C (hUBC) were evaluated using the primers listed in Table 1 (Life Technologies), the SYBR Green Reaction Kit following suppliers' specifications (Roche), and measured by reverse transcription polymerase chain reaction (RT-PCR) in a Light Cycler 480 device (Roche). Gene expression levels were normalized using a factor derived from the equation √(Ywhaz x hUBC). Crossing points were assessed using the Light Cycler software (version 4) and plotted versus serial dilutions of cDNA derived from a human universal reference total RNA (Clontech Laboratories Palo Alto, CA, USA).

Statistical analysis

Three independent experiments were performed in duplicate, and data are expressed as mean ± standard deviation (SD). Statistical analysis was performed using one-way analysis of variance (ANOVA) followed by Tukey–Kramer's post hoc test (Prism version 5.02, GraphPad Software Inc., La Jolla, CA, USA). Differences were considered significant at the 5% level ($p<0.05$).

Table 1. Primer sequences used for RT-PCR

Target gene		Oligonucleotide sequence	Annealing temperature (°C)	Product Size (bp)
Col 1α1	Forward	5' TCCAACGAGATCGAGATCC 3'	57	191
	Reverse	5' AAGCCGAATTCCTGGTCT 3'		
Col 3α1	Forward	5' GATCCGTTCTCTGCGATGAC 3'	56	279
	Reverse	5' AGTTCTGAGGACCAGTAGGG 3'		
MMP-2	Forward	5' GGCAGTGCAATACCTGAACA 3'	56	253
	Reverse	5' AGGTGTGTAGCCAATGATCCT 3'		
TIMP-2	Forward	5' CTGAACCACAGGTACCAGAT 3'	63	237
	Reverse	5' TGCTTATGGGTCCTCGATG 3'		
Ywhaz	Forward	5' GATGAAGCCATTGCTGAACTTG 3'	56	229
	Reverse	5' CTATTTGTGGGACAGCATGGA 3'		
hUBC	Forward	5' GCGGTGAACGCCGATGATTAT 3'	56	202
	Reverse	5' TTTGCCTTGACATTCTCGATGG 3'		

Col1α1, α1(I)procollagen; Col3α1, α1(III)procollagen; MMP-2, matrix metalloproteinase 2; TIMP-2, tissue inhibitor of metalloproteinases 2; hUBC, human ubiquitin C; Ywhaz, tyrosine 3-monooxygenase/tryptophan 5-monooxygenase activation protein, zeta polypeptide.

RESULTS

After 48h of cyclic mechanical loading, morphological analysis showed cell alignment perpendicular to the force that was facilitated by collagen-coated surfaces, with no apparent differences between healthy (Fig.1b and d) and POP (Fig.2c and d) fibroblasts. At an earlier time point (24h), load-induced rearrangement of F-actin fibers was completed for mild but not severe POP fibroblasts (Fig.2a vs. b). Static control cells displayed random distribution independent of surface (Fig.1a and b).

To evaluate the effects of the different experimental conditions on the capacity of the fibroblasts to remodel the ECM, secreted MMP-2 and MMP-9 enzymatic activity were evaluated at two time points (24 and 48h). Total levels of released MMP-2 by POP fibroblasts at 24h were lower than healthy control cells, independent of the surface substrate (Fig.3a). At the same time point, but only on uncoated plates, cyclic mechanical loading induced activation of MMP-2, which was more pronounced in healthy fibroblasts. Under static conditions, MMP-2 activation was only observed in healthy control cells on uncoated plates (Fig.3a left blot). There was no apparent activation of MMP-2 on collagen-I-coated plates, with the exception of a very faint band of active MMP-2 on stretched mild POP fibroblasts (Fig.3a middle blot).

At a later time point (48h), levels of released pro-MMP-2 were similar on collagen-I surfaces, and no active MMP-2 was found (Fig.3b middle blot). On uncoated plates, stretching of fibroblasts induced MMP-2 activation that increased from 24 to 48h.

Such activation was lower in POP fibroblasts compared with healthy controls (Fig.3b and b, left blot). Western blot analysis at 48h revealed the presence of TIMP-2 only in cells exposed to collagen-coated plates without any apparent regulation by loading (Fig.3c). Released MMP-9 was below detection levels.

As levels of released MMP-2 were higher after 48h, these data were quantified and normalized to total protein content. Quantitative data revealed that under static conditions and regardless of the type of substrate, most cells released similar amounts of pro-MMP-2 into the extracellular environment (Fig.3d and e). On uncoated plates, mechanical loading induced MMP-2 activation by all cell populations, as the ratios between active and inactive (pro) MMP-2 forms were always >1, and ANOVA showed that such an increment was significant only in the case of healthy fibroblasts ($p<0.01$) (Fig.3f). On collagen-I-coated plates, quantitative data revealed similar expression profiles of pro-MMP-2 and TIMP-2 in all groups (Fig.3e and g).

To detect differences at the gene-expression level, ECM remodelling-related genes Col1a1, Col3a1, MMP-2, and TIMP-2 were chosen to evaluate the effects of cyclic mechanical loading and surface substrate after 48h of treatment. On uncoated plates, both mild and severe POP fibroblasts showed significantly lower gene expression of Col1a1 and Col3a1 when compared with healthy controls (Fig.4a and b). On the same substrate, gene expression of Col1α1 was down-regulated by mechanical loading in healthy but not in POP fibroblasts. MMP-2 expression levels were similar in all fibroblasts, independent of loading conditions (Fig.4c and d). On collagen-I-coated plates, mild but not severe POP fibroblasts showed lower gene expression levels of Col1a1, Col3a1, and MMP-2 when compared with healthy controls (Fig.4e, f and g). TIMP-2 expression levels were similar in all fibroblasts, independent of loading or coating conditions (Fig.4h).

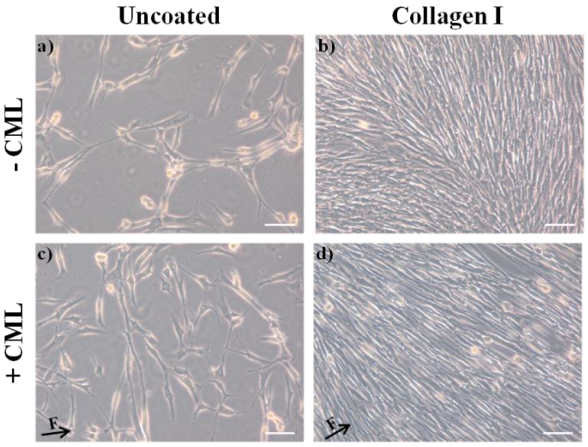

Figure 1. Cell attachment and alignment is facilitated by collagen I substrates. Representative images of healthy fibroblasts after 48h of cyclic mechanical loading (CML) on uncoated (**a** and **c**) or collagen I-coated (**b** and **d**) plates. Morphology shows random cell distribution under static conditions (-CML, **a** and **b**); whereas stretching induced cell alignment perpendicular to the force (F), especially on collagen I-coated plates (+CML, **c** and **d**). Images were acquired with 10x objective of a Leica microscope, bar is 100µm.

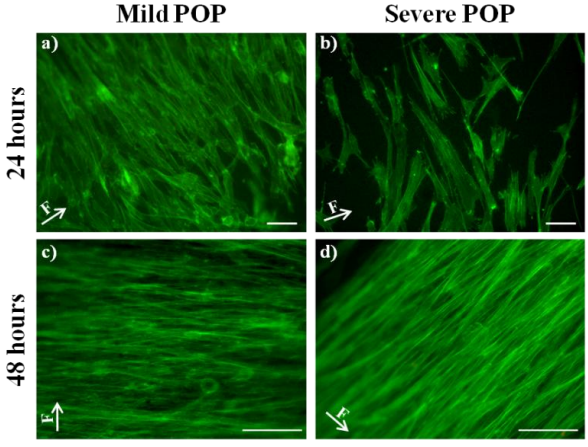

Figure 2. On collagen I-coated plates, rearrangement of F-actin fibres was completed after 24h of loading for mild but not for severe POP fibroblasts. Representative images of POP fibroblasts F-actin fibres showing cell alignment perpendicular to the force (F) on collagen I-coated plates after 24h (**a** and **b**) or 48h (**c** and **d**) of loading. F-actin fibres stained with phalloidin, bar is 100µm.

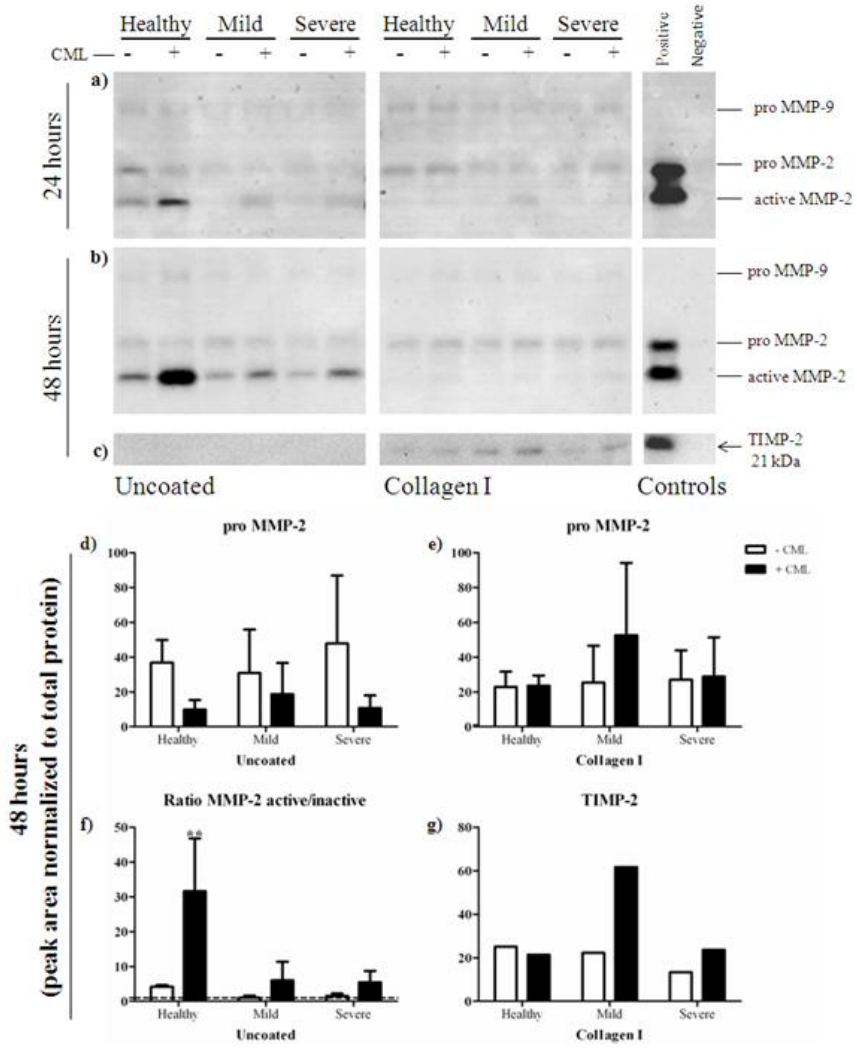

Figure 3. Mechanical loading induced activation over time of MMP-2 by fibroblasts seeded on uncoated plates. Conditioned media of fibroblasts from healthy, mild and severe POP patients after 24h **(a)** or 48h (**b** and **c**) of cyclic mechanical loading (CML) on uncoated or collagen I-coated plates was evaluated. Blots **(a)** and **(b)** are representative zymograms showing MMP-2 activity. **(c)** is a western blot of conditioned media (concentrated 2x) showing that TIMP-2 was released by the cells only on collagen substrates. Blots at 48h of CML were analysed with imageJ and quantitative data was normalised to total protein content. Quantitative data from zymograms show: levels of released pro MMP-2 by fibroblasts on uncoated **(d)** or collagen I-coated **(e)** plates; and the ratio between active and inactive MMP-2 forms on uncoated plates (**f**). Data represent the mean ± SD. **p<0.01 compared to static condition (- CML). Graph **(g)** corresponds to the release of TIMP-2 by fibroblasts on collagen substrates. Low serum media which was not exposed to cells was used as negative control. Positive controls used: for zymograms was human-recombinant MMP-2 and for western blot was cell lysates from dermal stem cells.

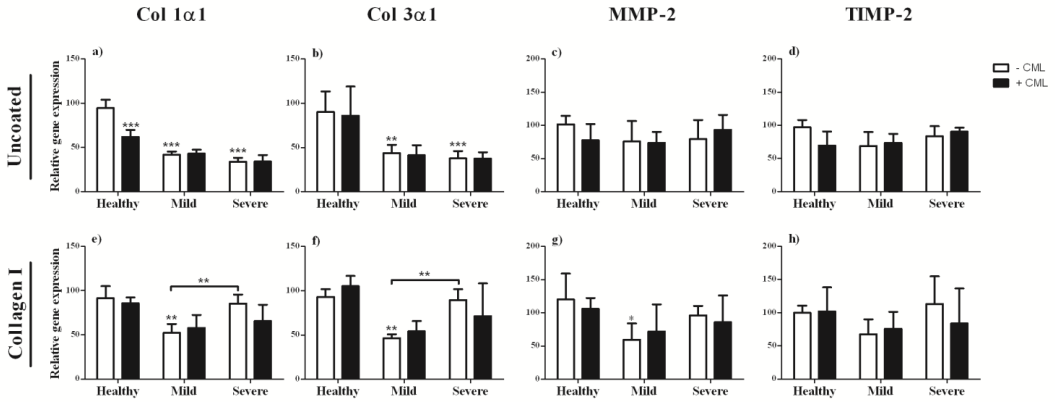

Figure 4. Relative expression of extracellular matrix remodelling related genes. Fibroblasts from healthy, mild or severe POP patients were subjected, or not subjected, to cyclic mechanical loading (+/- CML) on uncoated (**a**, **b**, **c** and **d**) or collagen I-coated plates (**e**, **f**, **g** and **h**). Each column represents a different gene: Col 1α1 **(a)** and **(e);** Col 3α1 **(b)** and **(f)**; MMP-2 **(c)** and **(g)**; TIMP-2 **(d)** and **(h)**. Values are normalized to housekeeping genes (Ywhaz and hUBC), expressed as a percentage of healthy control and represent the mean ± SD. *p<0.05, **p<0.01, ***p<0.001; compared to the first bar unless indicated otherwise.

DISCUSSION

In POP, tissue strength is lost, stiffness is increased[9–11], and ECM quality is compromised[15]. Consequently, fibroblasts might be exposed to an abnormal matrix. The biomechanical environment may be further compromised if during pelvic reconstructive surgery, stiff, nonresorbable polymeric mesh is used to replace tissue function. We evaluated the possible roles of CML and two surface substrates on the functionality of healthy and mild and severe POP fibroblasts using an *in vitro* dynamic model. We found variations of fibroblast responses at morphological, enzymatic, and gene expression levels.

Cells respond to mechanical stimuli by remodelling their actin cytoskeleton[20]. Our results show that all fibroblasts were mechanoresponsive, as their actin cytoskeleton aligned perpendicular to the force after 48h of cyclic mechanical loading, especially in the presence of collagen I. This finding is consistent with previous reports that fibroblasts from the pelvic floor completely align after being stretched for 48 h[21]. Differences between cell populations were seen after 24h of loading on collagen-I substrates, when visualization of actin filaments revealed that alignment of severe POP fibroblasts appear delayed in comparison with their mild counterparts; also, released MMP-2 was lower in fibroblasts from POP patients compared with healthy control cells. These effects seemed to disappear with time, as after 48h of stretching, there was no apparent difference in cell alignment, no activation of MMP-2, TIMP-2 protein levels corresponded to pro-MMP-2, and no difference in gene expression of MMP-2 or TIMP-2.

Interestingly, when fibroblasts were exposed to artificial polymeric substrates (uncoated plates), clear differences were seen in production and activation of MMP-2, TIMP-2 could not be detected, and mechanical loading promoted MMP-2 activation over time. After 48h of loading, MMP-2 activation was significant only in healthy, not in POP, fibroblasts. Moreover, cells from women with prolapse showed differential gene expression of anabolic but not catabolic compounds: collagens I and III were lower in women with POP, and mechanical loading down-regulated collagen I on healthy fibroblasts only. Changes seen with catabolically secreted proteins were not correlated at gene expression levels. Such discrepancy emphasizes the importance of using different evaluation parameters because changes at gene expression levels do not necessarily reflect changes at protein levels, and they can occur at different times.

Taken together, our data suggest that although fibroblasts from POP patients seem to have lower mechanoresponses, in the presence of collagen-I substrate, the system eventually reaches a balance. This latter finding confirms 48h data from Zong and colleagues[22], who used collagen-I-coated plates in their dynamic *in vitro* model with similar experimental conditions (sinus wave; amplitudes 8% and 16%; frequency 1 Hz), and found no differences between healthy and mild and severe POP vaginal fibroblasts. However, it appears that when cells are exposed to artificial polymeric substrates and stress is imposed, this balance is not reached. Fibroblasts from women with POP seem preconditioned by the abnormal prolapsed matrix. Unable to respond in the same way as control cells, POP fibroblasts might not be able to restore ECM homeostasis when artificial polymeric substrates are added to their microenvironment. In such circumstances, tissue remodelling might not be restored but, rather, may in turn provide a negative feedback loop that deteriorates the ECM even further, leading to an additional loss of strength, increased stiffness, and eventually more tissue damage. Such implications at the micro level are in line with findings at the macro level. Several studies report increased stiffness in prolapsed tissues when assessing biomechanical properties of the vaginal wall from patients with POP compared with healthy controls[17–19]. Moreover, it has also been shown that polymeric mesh used in genital prolapse surgery is stiffer than native tissue[23]. Feola and colleagues[24] showed correlation between mesh stiffness and tissue deterioration in a nonprimate animal model. Therefore, changes in the vaginal wall at the cellular level could be good indicators of tissue behavior and should be taken into account when using polymeric mesh to treat patients. As surface substrate affects cellular behavior, and cell–matrix interactions seem to be impaired in POP fibroblasts, improving mesh surface characteristics could enhance implant integration.

Conclusions from this study should be treated with care: results were obtained in an *in vitro* set-up, which allowed us to control certain parameters but does not fully reflect the *in vivo* situation. Furthermore, we are aware that our patient population was too small to draw conclusions about all women with POP. The experiments were repeated three times, all confirming the first results and suggesting our model is valid. We are in the process of expanding our sample size.

To improve pelvic floor treatment, further studies evaluating the effect on fibroblasts of different ECM proteins in dynamic *in vitro* systems could provide important clues to improve mesh designs before using animals for *in vivo* studies and humans for clinical trials. This approach should provide better clinical outcomes by using information from bench to bedside to restore pelvic support and improve host–implant integration when treating POP.

In summary, this study provides a model by which to evaluate dynamic interactions of fibroblasts from the pelvic floor with artificial substrates *in vitro*. Unlike previous models[21,22], we chose a continuous physiological stretching regimen to compare fibroblast mechanoresponses to artificial collagen-I-coated and uncoated substrates. We thereby show clear differences between POP and healthy fibroblasts on artificial polymer substrates. This emphasizes the importance of evaluating cell-matrix interactions with different surroundings to better understand the influences in dynamic environments of proteins from the ECM on vaginal fibroblast behavior. Such outcomes may provide important clues for designing biomesh that appropriately mimics the ECM environment, as it seems that the addition of collagen coating helps restore vaginal-wall metabolic balance. This new approach may thus improve treatment for POP.

Acknowledgements AM Ruiz-Zapata acknowledges financial support from Advanced Technologies and Regenerative Medicine (ATRM, LLC), a Johnson & Johnson company, and by a grant from the Dutch government to The Netherlands Institute for Regenerative Medicine (NIRM, grant No. FES0908).

REFERENCES

1. Jelovsek JE, Maher C, Barber MD (2007) Pelvic organ prolapse. The Lancet 369:1027-1038.
2. Mosier E, Lin VK, Zimmern P (2010) Extracellular matrix expression of human prolapsed vaginal wall. Neurourol Urodyn 29:582-586.
3. U.S. Food and Drug Administration FDA (2011) Urogynecologic surgical mesh: update on the safety and effectiveness of transvaginal placement for pelvic organ prolapse. IOP FDAWeb. http://www.fda.gov/downloads/medicaldevices/safety/alertsandnotices/UCM262760.pdf. Accessed 12 November 2012.
4. Keys T, Campeau L, Badlani G (2012) Synthetic mesh in the surgical repair of pelvic organ prolapse: current status and future directions. Urology 80:237-243.
5. Kerkhof MH, Hendriks L, Brölmann HAM (2009) Changes in connective tissue in patients with pelvic organ prolapse--a review of the current literature. Int Urogynecol J Pelvic Floor Dysfunct 20:461-474.
6. Feola A, Barone W, Moalli P, Abramowitch S (2012) Characterizing the ex vivo textile and structural properties of synthetic prolapse mesh products. Int Urogynecol J DOI 10.1007/s00192-012-1901-1.
7. Moalli PA, Shand SH, Zyczynski HM, Gordy SC, Meyn LA (2005) Remodeling of vaginal connective tissue in patients with prolapse. Obstet Gynecol 106:953-963.
8. Bortolini MA, Shynlova O, Drutz HP et al (2011) Expression of bone morphogenetic protein-1 in vaginal tissue of women with severe pelvic organ prolapse. Am J Obstet Gynecol 204:544.e1-8.
9. Jean-Charles C, Rubod C, Brieu M, Boukerrou M, Fasel J, Cosson M (2010) Biomechanical properties of prolapsed or non-prolapsed vaginal tissue: impact on genital prolapse surgery. Int Urogynecol J 21:1535-1538.
10. Martins P, Silva-Filho AG, Maciel da Fonseca AMR, Santos A, Santos L, Mascarenhas T, Jorge RMN, Ferreira AJM (2012) Biomechanical properties of vaginal tissue in women with pelvic organ prolapse. Gynecol Obstet Invest DOI 10.1007/s00192-012-1901-1.

11. Zhou L, Lee JH, Wen Y, Constantinou C, Yoshinobu M, Omata S, Chen B (2012) Biomechanical properties and associated collagen composition in vaginal tissue of women with pelvic organ prolapse. J Urol 188(3):875-880.
12. Phillips CH, Anthony F, Benyon C, Monga AK (2006) Collagen metabolism in the uterosacral ligaments and vaginal skin of women with uterine prolapse. BJOG 113:39-46.
13. Liang CC, Huang HY, Tseng LH, Chang SD, Lo TS, Lee CL (2010) Expression of matrix metalloproteinase-2 and tissue inhibitors of metalloproteinase-1 (TIMP-1, TIMP-2 and TIMP-3) in women with uterine prolapse but without urinary incontinence. Eur J Obstet Gynecol Reprod Biol 153:94-98.
14. Berger MB, Ramanah R, Guire KE, Delancey JOL (2012) Is cervical elongation associated with pelvic organ prolapse? Int Urogynecol J 23:1095-1103.
15. Word RA, Pathi S, Schaffer JI (2009) Pathophysiology of pelvic organ prolapse. Obstet Gynecol Clin North Am 36:521-539.
16. Jackson SR, Eckford SD, Abrams P, Avery NC, Tarlton JF, Bailey AJ (1996) Changes in metabolism of collagen in genitourinary prolapse. The Lancet 347:1658-1661.
17. Budatha M, Roshanravan S, Zheng Q et al (2011) Extracellular matrix proteases contribute to progression of pelvic organ prolapse in mice and humans. J Clin Invest 121:2048-2059.
18. Blaauboer ME, Smit TH, Hanemaaijer R, Stoop R, Everts V (2011) Cyclic mechanical stretch reduces myofibroblast differentiation of primary lung fibroblasts. Biochem Biophys Res Commun 404:23-27.
19. Perez-Amodio S, Beertsen W, Everts V (2004) (Pre-)osteoclasts induce retraction of osteoblasts before their fusion to osteoclasts. J Bone Miner Res 19:1722-1731.
20. Kong D, Ji B, Dai L (2008) Stability of adhesion clusters and cell reorientation under lateral cyclic tension. Biophys J 95:4034-4044.21. Ewies AAA, Elshafie M, Li J et al (2008) Changes in transcription profile and cytoskeleton morphology in pelvic ligament fibroblasts in response to stretch: the effects of estradiol and levormeloxifene. Mol Hum Reprod 14:127-135.
22. Zong W, Jallah ZC, Stein SE, Abramowitch SD, Moalli PA (2010) Repetitive mechanical stretch increases extracellular collagenase activity in vaginal fibroblasts. Female Pelvic Med Reconstr Surg 16:257-262.
23. Ozog Y, Kostantinovic M, Werbrouck E, De Ridder D, Mazza E, Deprest J (2011) Persistence of polypropylene mesh anisotropy after implantation: an experimental study. BJOG 118:1180-1185.
24. Feola A, Abramowitch S, Jallah Z, Stein S, Barone W, Palcsey S, Moally P (2013) Deterioration in biomechanical properties of the vagina following implantation of high-stiffness prolapse mesh. BJOG 120:224-232.